# Laser-Induced Fluorescence Measurements on the Plume from a 1 kW Arcjet Operated on Simulated Ammonia

W. M. Ruyten*
*University of Tennessee-Calspan*
*Center for Space Transportation and Applied Research*
*Tullahoma, Tennessee 37388-8897*

and

D. Burtner† and D. Keefer**
*Center for Laser Applications*
*University of Tennessee Space Institute*
*Tullahoma, Tennessee 37388-8897*

## Abstract

*We report the results of laser induced fluorescence measurements on the plume from a 1 kW arcjet operated on simulated ammonia. The measurements were performed on the Balmer-alpha line of atomic hydrogen. The results are shown to be in essential agreement with earlier spectroscopic measurements on the same line. For example, both measurements indicate that the plume is underexpanded. The agreement between the two types of measurements demonstrates that, surprisingly, emission spectroscopy can be used as a valuable tool for measuring plume velocities. We also compare the experimental results with those from a numerical simulation based on equilibrium chemistry. The numerical results overestimate the exit velocities and temperatures significantly, indicating that nonequilibrium effects need to be incorporated into the code.*

## 1. Introduction

There have been substantial efforts over the last several years to gain a better understanding of arcjet operation using both experimental and numerical approaches. Here we give a concise report of activities at UTSI and CSTAR involving experimental research and numerical modeling of a 1 kW arcjet operated on (simulated) ammonia propellant. In particular, we compare the results obtained with different techniques (emission spectroscopy and laser-induced fluorescence—both on the hydrogen Balmer-alpha line) and we compare the experimental data with calculated results from a code which employs equilibrium chemistry.

* Senior Engineer, member AIAA
† Graduate Research Assistant, student member AIAA
** B. H. Goethert Professor of ES&M; member AIAA

## 2. Experimental work

Experimental measurements were performed on a 1 kW arcjet thruster from NASA Lewis Research Center. The only modification from the standard design [1] was the use of a nozzle with a 0.50 mm constrictor diameter. A 1:3 nitrogen-hydrogen mixture was used as propellant. A standard operating condition was chosen with a flow rate of 6.0 slm (38 mg/s), resulting in a background pressure of 130 Pa (1.0 Torr). Typical values of arc current and arc voltage were 10.0 A at 108 V.

### 2.1 Emission spectroscopic measurements

Using a SPEX 1.25 m spectrometer, we performed a series of spectroscopic measurements on the Balmer-lines of atomic hydrogen, and on the $c \rightarrow b$ band of the NH radical at 450 nm. The results of

these measurements are reported in [2]. For the purpose of comparison with the laser-induced fluorescence measurements, we summarize the results of the velocity- and temperature-measurements on the hydrogen Balmer-alpha line at 656.3 nm.

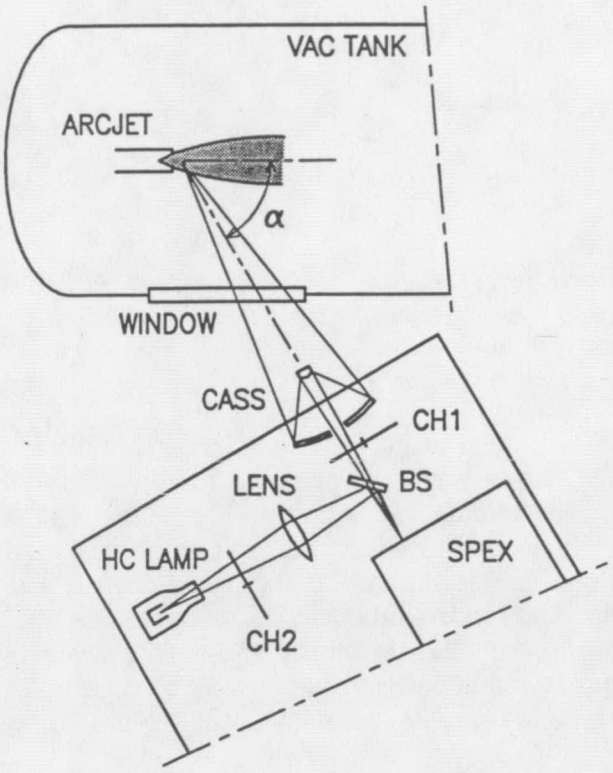


**Figure 1:** Experimental setup for the spectroscopic measurements. The optics are positioned at a nonorthogonal angle to the plume centerline to allow a determination of the Doppler shift of the flow.

Figure 1 shows the experimental setup. Using a cassegrain telescope, light from the plume was focused on the entrance slit of a SPEX 1.25 m spectrometer equipped with an 1800 gr/mm grating. Typically, data were taken at an instrument resolution of 0.12 Å fwhm. By comparison, the observed widths of the H-alpha lines were on the order of 0.4 Å fwhm. Light from a hollow cathode lamp containing hydrogen buffer gas was collected simultaneously with the plume signal to allow a calibration of the Doppler shift of the latter. The signals from the arcjet plume and the hollow cathode lamp were separated using dual lock-in detection.

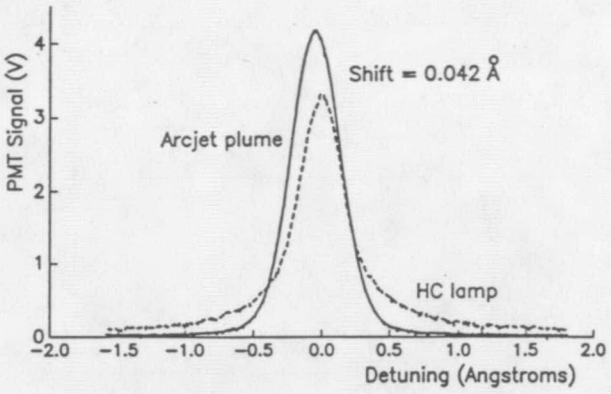


**Figure 2:** Example of a scan of the hydrogen Balmer-alpha line, in which the signals from both the plume and the hollow cathode lamp are shown.

A typical scan of the H-alpha line is shown in Fig. 2. The relative shift between the two line centers is essentially the Doppler shift which results from the plume motion. By curve-fitting the observed line shapes, it was possible to determine this shift to an accuracy on the order of one percent of the spectrometer line width, or about 0.0015 Å. However, as explained in [3], a calibration procedure had to be employed in which the apparent shifts were corrected by the values measured in an orthogonal observation geometry (we attribute these apparent shifts—which are smaller than the instrument width—to different alignments of the plume and the hollow cathode lamp relative to the grating).

Results of these plume velocity measurements are shown in Fig. 3. The ``average" position of the arcjet exit plane, defined as the intersect between the line-of-sight direction and the plume centerline, is at an axial coordinate of 2.5 mm, as is indicated in Fig. 4. At this position, the measured velocity of the plume is 4070 ± 80 m/s for an arc current of 10 A. However, the velocity increases to 5500 m/s at a position 3 mm downstream from the exit plane and appears to plateau at this value. We show in Section 2.2 that this behavior is consistent with that observed using laser-induced fluorescence measurements.

We also obtained temperature data from the Balmer-alpha scans. These values were obtained by fitting the line profiles, taking into account explicitly the measured instrument profile, the fine-structure of the Balmer-alpha line, and electron Stark-broadening (significant only for measurements upstream of the

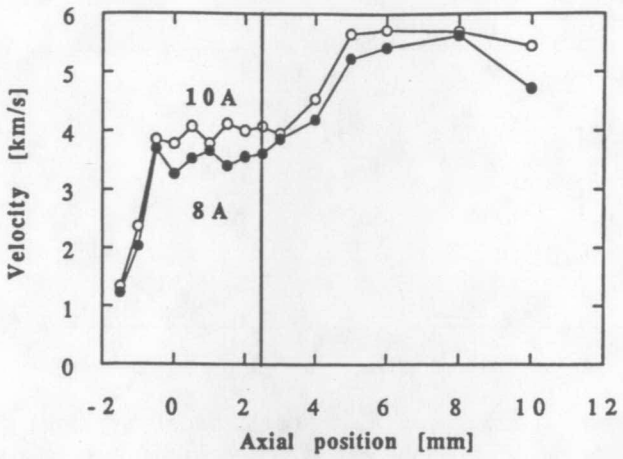


**Figure 3:** Measured plume velocities as a function of axial position in the flow. The axial coordinate is to be interpreted according to Fig. 4.

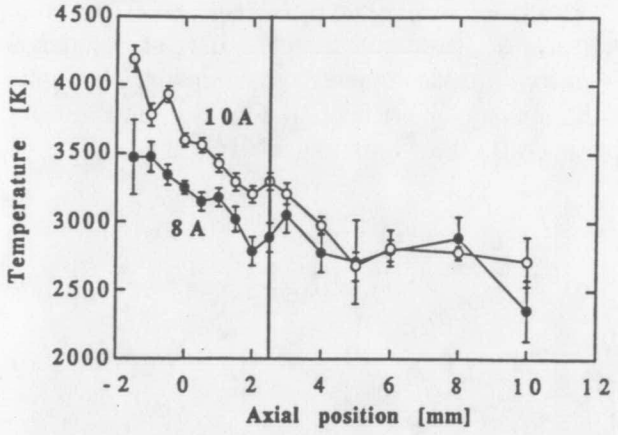


**Figure 5:** Temperatures calculated on the basis of the fitted Doppler widths of the emission data for the hydrogen Balmer-alpha line.

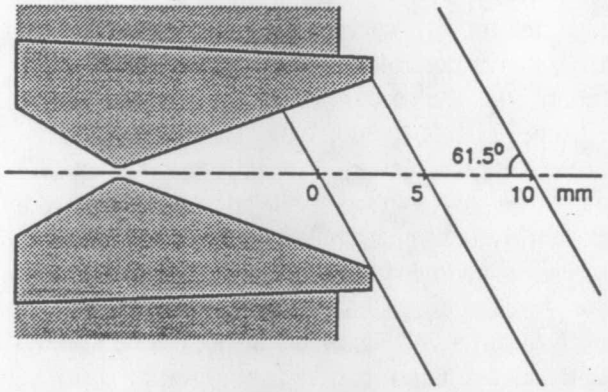


**Figure 4:** Schematic of the observation geometry close to the arcjet nozzle. The choice of the axial coordinates is such that the exit plane is located at a position of 2.5 mm.

average exit plane location [2]). Results of these temperature determinations are shown in Fig. 5. As expected, the temperature drops as the plume expands. For a current of 10 A, a temperature of about 3250 K is found at the average exit plane location. This value turns out to be significantly higher than that obtained from the spatially resolved laser-induced fluorescence measurements, probably as a result of integrating over the radial velocity distribution in the plume in the emission measurements.

We also determined the rotational temperature of the c → b band of the NH radical and the temperature which results from an analysis of the intensity ratio of the Balmer-alpha and -beta lines. The former was roughly constant around 2700 K throughout the region shown in Figs. 3 and 4. The latter increased from 2500 K at an axial position of 0 mm in Figs. 3 and 4 to a value of 4000 K at 8 mm. This result clearly indicates that emissions from the excited states of atomic hydrogen are not in thermal equilibrium and that the derived value is not a reliable indicator of the plume temperature.

## 2.2 Laser-induced fluorescence measurements

Laser-induced fluorescence (LIF) measurements were performed using a setup which had been employed previously to measure velocities in an argon arcjet plume [4,5]. A schematic of the experimental setup is shown in Fig. 6. The beam from a frequency-stabilized dye laser is split and focused into the arcjet plume in such a way that one beam intersects the plume perpendicular to the plume axis and one beam is offset from the orthogonal direction by about 14 degrees. Previously, this was accomplished by focusing two parallel beams with a single lens. However, the resulting beam waists were small enough that saturation of the optical signal occurred at the maximum available laser power level. Thus, an alternative setup was chosen in which the beams were focussed with an extremely long-focal-length lens outside the vacuum chamber, and beam-steering of the 14-degree-off-perpendicular beam was achieved with a mirror inside the chamber. The

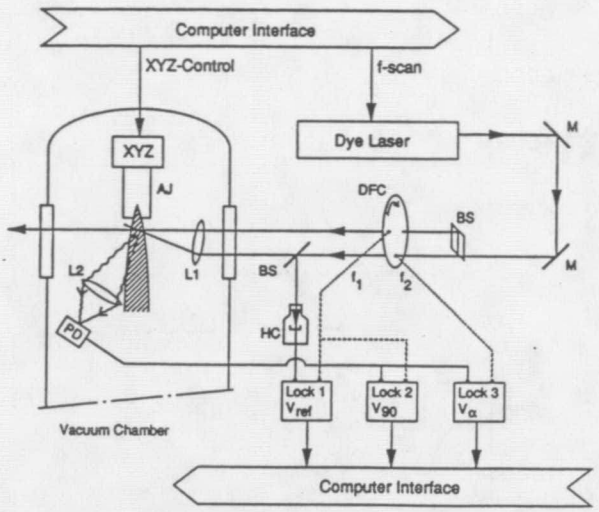


**Figure 6:** Experimental setup for the laser-induced fluorescence measurements.

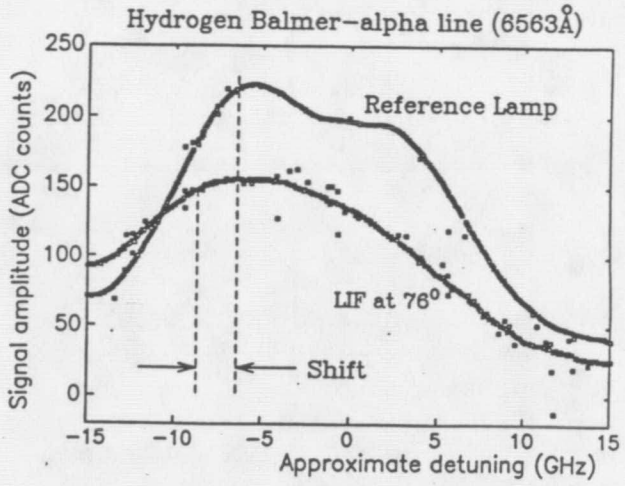


**Figure 7:** Typical LIF scan of the hydrogen Balmer-alpha line. The Doppler shift between the plume signal and the reference signal is indicated.

resulting beam waists were much larger (on the order of 1 mm), thereby eliminating the saturation problem. However, a new complication of this approach was an increased level of scattered laser light on the detector.

As before, the detector was a photo-diode, mounted inside the vacuum chamber. Light from the plume was collected by a lens which was mounted perpendicular to the plane in which the two laser beams were crossed. A pinhole on the photo-diode was used to confine the observation region to a spot with a diameter equal to that of the laser beams, on the order of 1 mm. This setup proved quite adequate for the earlier measurements on the argon arcjet plume. However, a smaller signal-to-noise signal resulted in the present measurements on the hydrogen Balmer-alpha line. Thus it would be desirable to repeat the measurements with a more sensitive detector (that is, a photo-multiplier tube), mounted outside of the chamber [6].

Figure 7 shows a typical scan of the Balmer-alpha line, showing one of the two LIF signals and the reference signal, obtained from the hollow cathode lamp through the optogalvanic effect. Because of the much narrower instrument width of the laser (1 MHz) as compared to the emission measurements (0.12 Å or 8400 MHz), and because the lack of averaging over radial velocity gradients in the LIF measurements, the spectral width of the LIF signal is significantly less than that of the emission signal, thereby revealing the fine-structure of the Balmer-alpha line. On the other hand, the scan width of the laser system (30 GHz, or about 0.43 Å) was not sufficient to cover more much than just the central part of the line shape in a single scan.

Using gaussian curve fits which accounted for the fine structure, line centers and line widths were extracted from each of the LIF measurements. Unlike for the emission measurements, no corrections to the line center determinations of the hollow-cathode data were necessary, and the Doppler shifts were calculated simply as the difference between the fitted line centers of the plume data and the data from the hollow cathode lamp. The resulting shifts were converted to radial and axial components of the plume flow velocities.

Results of these measurements are shown in Figs. 8 and 9. Figure 8 shows vector velocities measured at a number of positions in the plume, at axial positions of 1 mm, 2.5 mm, and 4 mm downstream from the exit plane and at several radial locations for each of these axial positions. Because of the reasons mentioned above (not enough sensitivity of the detector; a significant background signal due to laser scatter as a result of using 1 mm wide beams; limited

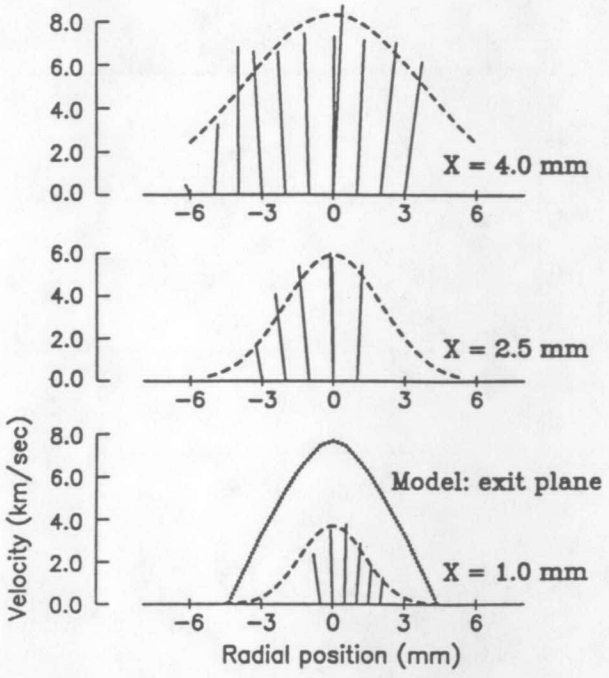


**Figure 8:** Vector velocities in the arcjet plume, obtained from the LIF measurements at different downstream positions in the plume. The dashed lines are added to emphasize the trend of the data. Also shown are the numerical results at the exit plane.

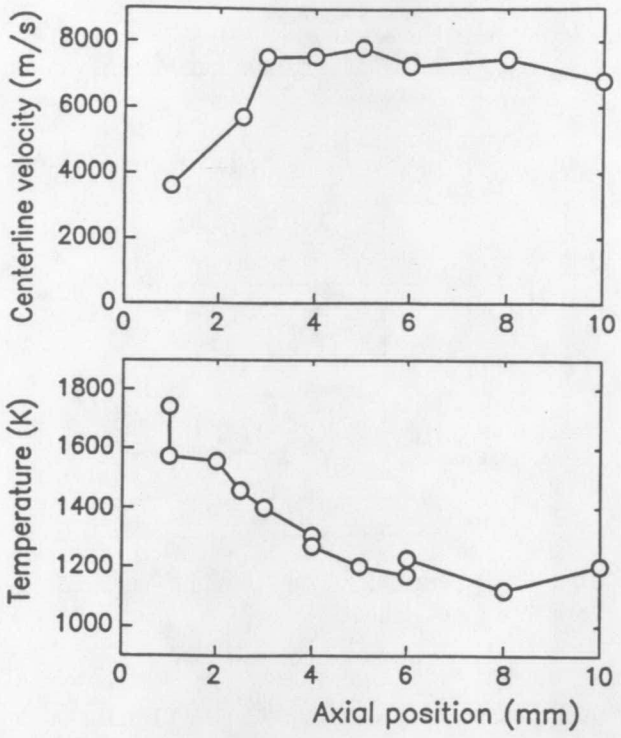


**Figure 9:** Axial velocities (a) and temperatures (b) measured on centerline by the LIF technique.

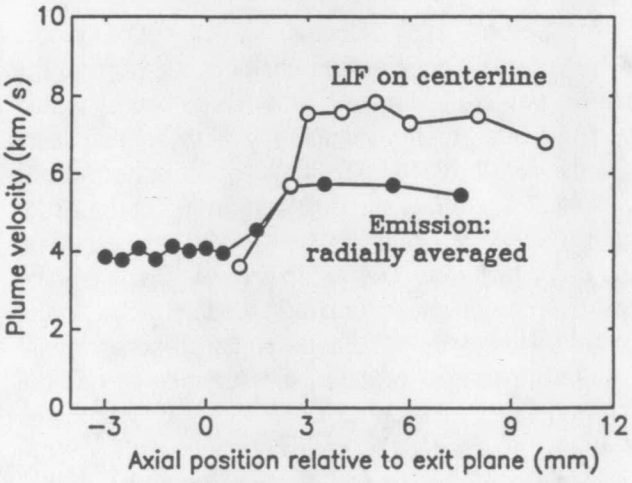


**Figure 10:** Comparison of axial velocity data obtained with LIF and emission spectroscopy.

scan range on the laser), the data are not of the same quality as those obtained in our earlier work [4, 5] or those obtained by Liebeskind et al. on the same spectral line in a hydrogen arcjet plume [6]. However, the trend of the data (which is emphasized by the dashed lines in Fig. 8) is quite clear: The plume velocity is largest on centerline, and increases dramatically from the 1 mm position (with a peak velocity of about 4 km/s) to the 4 mm position (with a peak velocity of 8 km/s—see also Fig. 9a). This is fundamentally the same result as that obtained in the emission measurements, namely that the flow accelerates upon exiting the thruster. Moreover, because the emission data are averaged over the radial extent of the plume, it seems quite reasonable that the velocities measured on centerline using LIF exceed those measured in the emission measurements. Figure 10 displays the LIF velocity data and the velocity data from the emission measurements in one figure to emphasize the qualitative agreement between the two sets of data (the axial coordinates of the emission data were adjusted so that the zero-position on the horizontal axis indicates the actual position of the nozzle exit plane for both sets of data).

The essential agreement between the line-of-sight-averaged emission spectroscopic measurements and the point-resolved laser-induced fluorescence measurements is especially significant in that it is a demonstration of the ability to obtain plume velocity data using emission spectroscopy. Against the obvious shortcoming that the emission data are line-

of-sight averages stands the advantage that the equipment to perform emission measurements is much less complex and costly, so that it is available to more researchers. Also, emission spectroscopy offers greater flexibility in measuring the plume velocities of multiple species in the plume (for example, in [2] we verified that the same plume velocities were obtained for the hydrogen Balmer-alpha, -beta, and -gamma lines).

We also calculated temperature data from the fitted widths of the LIF profiles. Because of the large background signals which resulted from laser scatter in the experiment, and because of the limited scan range of the laser, the fitted widths were only accurate to about ten percent. Results on centerline are shown in Fig. 9b. As expected, the temperature drops as the plume expands. These LIF-derived values are significantly lower than those obtained from the emission measurements (cf. Fig. 5). The values obtained from the LIF measurements should be more accurate, because they do not involve averaging over the radial extent of the plume.

### 3. Numerical modeling results

The numerical model used in this work has been described fully in past papers [7, 8]. The algorithm is based on the Navier-Stokes solver, SIMPLE, developed by Gosman and Pun [9] and modified by Rhie [10] to handle both subsonic and supersonic flows.

The governing equations for steady, axisymmetric, compressible flow are solved in a transformed coordinate system which is a mapping of the true nonorthogonal and nonuniform r-z grid to a grid of unit squares. The program solves for five dependent variables. The axial, radial, and azimuthal velocity components, u, v, and w, are calculated from the three momentum equations. The static enthalpy, h, per unit mass is determined from the energy equation. Finally, the pressure, p, is obtained from the conservation of mass. The five equations are solved sequentially using updated values of the dependent variables as they become available and using the old values when the updated ones have not yet been calculated. Solution iterations continue until the residual errors have been reduced to reasonably small values. Stability is insured by using upwind differencing for convective terms and including fourth-order pressure smoothing.

The electromagnetic properties of the fluid are described by the azimuthal component of the magnetic field, $B_t$, which is obtained from an equation derived from Ohm's law. The radial and axial components of the magnetic field are assumed to be zero. The components of current ($J_z$ and $J_r$) are obtained from numerical derivatives of $B_t$. The total dissipated power is constrained to be equal to the prescribed power input.

The program is based on local thermodynamic equilibrium (LTE) and chemical equilibrium, so temperature and species concentrations are functions of static enthalpy and pressure only. Thermodynamic and transport properties are obtained from lookup tables organized by static enthalpy and pressure and are interpolated to obtain field point values. Local thermodynamic and chemical equilibrium were assumed in the construction of the lookup tables.

The computational grid is spanned by 51 axial and 31 radial points. The wall contours match those of the arcjet thruster. The walls are assumed to have a no-slip boundary condition and a zero normal pressure gradient. The variables v and w and the radial gradients of u, h, and p are set to zero on the center axis. Temperature, and therefore enthalpy, is specified on all walls. Enthalpy and mass flow are specified at the inlet, and inlet swirl is specified as a constant times the inlet velocity. It is assumed that the current flows from the cathode tip and uniformly enters the anode on the nozzle wall with no current-flow to the anode upstream of the diverging section and no current loops outside of the nozzle exit. This assumption allows the azimuthal magnetic field to be specified on all the computational boundaries. Since wall temperatures have not been experimentally determined, the wall temperatures used for the computation are estimates.

Operating parameters were chosen to correspond to those in the experiment (10 A, 108 V, and 38 mg/s). Calculated results for the flow velocities at the nozzle exit plane are shown in Figs. 11 and 12. The axial velocity data are also shown in Fig. 8, where

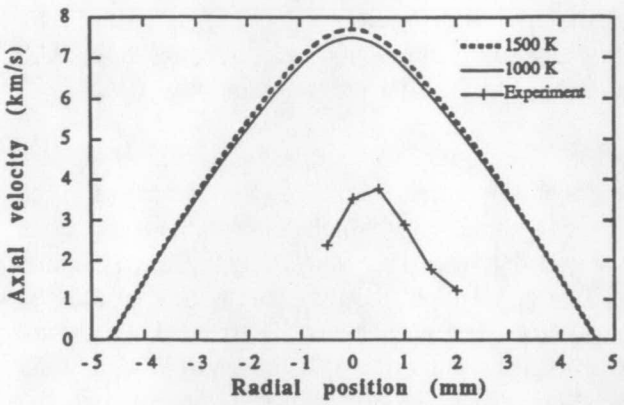


**Figure 11:** Calculated axial velocities at the exit plane. Results are shown for two wall-temperatures. Also shown are the results of the LIF measurements obtained 1 mm downstream from the exit plane.

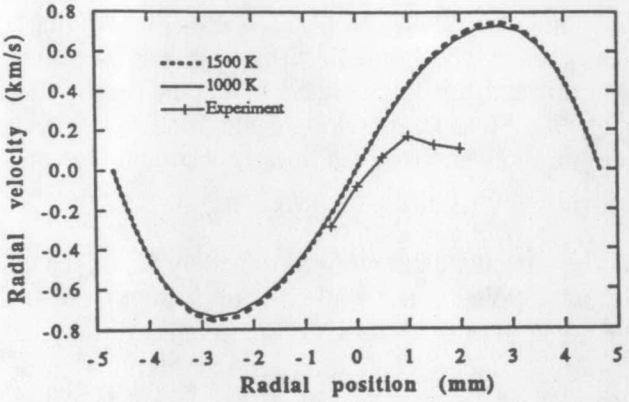


**Figure 12:** Same as Fig. 12 for the radial velocities.

they are displayed at the 1-mm measurement position. This was the closest distance from the exit plane for which LIF measurements could be performed, due to the relatively wide laser beam waists (1 mm diameter) used in the experiment. For comparison, the results of the LIF measurements (those taken at the 1-mm measurement location) are also shown in Figs. 11 and 12.

In comparing the calculated and measured data, it should be kept in mind that, 1 mm downstream from the exit plane, the outer edges of the flow experience effects of the expansion fan at the nozzle rim and effects of the shock wave caused by interaction of the flow with the 1-Torr background gas. The computer model calculates conditions at the nozzle exit assuming no interaction with an ambient gas. Therefore, the model and experiment should only be compared in the central region of the flow.

Even so, it is clear that the model greatly overpredicts the experimentally determined flow velocities, although the radial trend of the data is reproduced reasonably well. To assess the effect of the arcjet wall temperature, calculations were performed using two wall temperature files, based on nominal inlet temperatures of 1000 and 1500 Kelvin. Results of both calculations are shown in Figs. 11 and 12; they are seen to vary only slightly. Thus it is not likely that the choice of wall temperature has much bearing on the discrepancy between the calculated and experimental results.

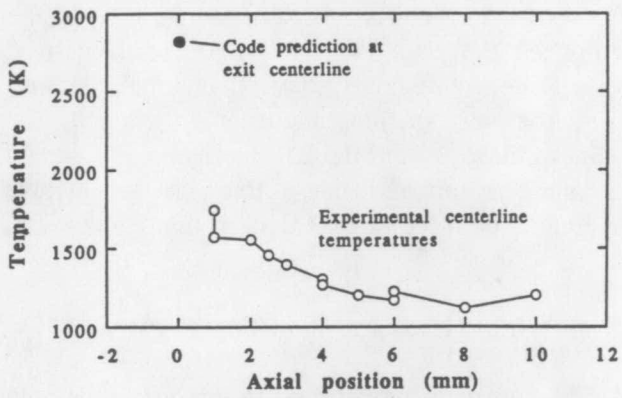


**Figure 13:** Calculated centerline temperature (single data point) shown with the experimental data from Fig. 9b.

The model also overpredicts the temperatures which were measured using LIF. This is shown in Fig. 13, in which the LIF data from Fig. 9b are reproduced. Also shown in Fig. 13 is the calculated temperature (on centerline) at the exit plane (the same temperature was found for both wall temperatures). The calculated value (2830 K) is about 1000 K higher than that which follows from an extrapolation of the LIF data to the exit plane.

In conclusion, the model overpredicts greatly the velocity as well as the temperature of the flow at the exit plane. We consider this result to be further evidence that the arcjet flow is not in thermal equilibrium. This conclusion has been drawn in other recent work on a 1-kW-class arcjet as well [10]. In particular, it appears that recombination losses in the nozzle cannot be neglected and that a

two-temperature model may be required to account separately for the difference in electron temperature and heavy-gas temperature. Since the electron temperature influences both the thermal conductivity and the electrical conductivity, such a two-temperature flow is expected to differ substantially from that of an equilibrium flow.

## 4. Conclusions

We have presented both experimental and numerical results on a 1 kW arcjet operated on simulated ammonia propellant. Results of plume velocity measurements using both emission spectroscopy and laser-induced fluorescence show fundamental agreement in that both indicate that the nozzle flow is underexpanded, despite the relatively high background pressure in the experiment. This results is not only significant per se, but it also points out the important fact that, somewhat surprisingly, emission spectroscopy can be a valuable diagnostic to measure plume velocities.

A comparison of the experimental results with those from a numerical model show that the numerical code, which is based on equilibrium chemistry in the arcjet flow, overestimates both the exit velocities and the exit temperatures of the arcjet flow. This result points out the need for further development of the numerical code, in which finite-rate chemistry and other nonequilibrium effects can be accounted for.

## Acknowledgments

This work was supported by grants from Rocket Research Company of Redmond, Washington; the Air Force Office of Scientific Research under grant AFOSR-91-0200; and by the Center for Space Transportation and Applied Research under NASA grant NAGW-1195. We gratefully acknowledge the loan of the arcjet system from NASA Lewis Research Center. Finally, we thank N. Wright for his expert technical assistance and R. Rhodes for assistance with the numerical model.

## References

[1] Curran, F. M., and Sarmiento, C. J., ``Low power arcjet performance characterization," AIAA paper 90-2578, Orlando, FL, July 1990.

[2] Ruyten, W. M., Burtner, D., and Keefer, D. ``Spectroscopic investigation of a low-power arcjet plume," AIAA paper 93-1790, Monterey, CA, June 1993.

[3] Ruyten, W. M., ``Velocity measurements in an electric thruster plume by emission spectroscopy," submitted to *Applied Optics*.

[4] Ruyten, W. M., and Keefer, D., ``Laser fluorescence velocimetry of an arcjet exhaust plume," paper 91-093, 22nd IEPC, Viareggio, Italy, October 1991.

[5] Ruyten, W. M., and Keefer, D., ``Characterization of electric thruster plumes using laser induced fluorescence measurements," AIAA paper 92-2965, Nashville, TN, July 1992.

[6] Liebeskind, J. G., Hanson, R. K., and Cappelli, M. A., ``Flow diagnostics of an arcjet using laser induced fluorescence," AIAA paper 92-3243, Nashville, TN, July 1992; see also AIAA paper 93-2530, Monterey, CA, June 1993.

[7] Rhodes, R. P. and Keefer, D., ``Numerical modeling of an arcjet thruster," AIAA 90-2614, 21st International Electric Propulsion Conference, Orlando, FL, June 1990.

[8] Rhodes, R. P. and Keefer, D., ``Modeling arcjet space thrusters," AIAA 91-1994, 27th AIAA/SAE/ASME/ASEE Joint Propulsion Conference, Sacramento, CA, June 1991.

[9] Gosman, A. D., and Pun, W. M., ``Calculation of recirculating flows," Report No. HTS/74/12, Dept. of Mechanical Engineering, Imperial College, London, 1974.

[10] Rhie, C. M., ``A pressure based Navier-Stokes solver," AIAA 86-0207, AIAA 24th Aerospace Sciences Meeting, Reno, NV, January 1986.

[11] Zube, D. M., and Auweter-Kurtz, M., ``Spectroscopic arcjet diagnostic under thermal equilibrium and nonequilibrium conditions," AIAA paper 93-1792, Monterey, CA, June 1993.